Osmane, A.; Dimmock, A.P.; Pulkkinen, Tuija I.

Universal properties of mirror mode turbulence in the Earth's magnetosheath

Published in:
Geophysical Research Letters

DOI:
10.1002/2015GL063771

Published: 01/01/2015

Document Version
Publisher's PDF, also known as Version of record

Please cite the original version:
Osmane, A., Dimmock, A. P., & Pulkkinen, T. I. (2015). Universal properties of mirror mode turbulence in the Earth's magnetosheath. *Geophysical Research Letters*, *42*(9), 3085-3092.
https://doi.org/10.1002/2015GL063771

AGU PUBLICATIONS

Geophysical Research Letters

RESEARCH LETTER
10.1002/2015GL063771

Key Points:
- Mirror modes in magnetosheath result in parabolic scaling of kurtosis-skewness
- Parabolic *K*-*S* collapse of mirror structures is a global magnetosheath constraint
- Parabolic relationship for mirror modes underlies universal turbulent properties

Correspondence to:
A. Osmane,
adnane.osmane@aalto.fi

Citation:
Osmane, A., A. P. Dimmock, and T. I. Pulkkinen (2015), Universal properties of mirror mode turbulence in the Earth's magnetosheath, *Geophys. Res. Lett.*, *42*, 3085–3092, doi:10.1002/2015GL063771.

Received 6 MAR 2015
Accepted 1 APR 2015
Accepted article online 7 APR 2015
Published online 4 May 2015

Universal properties of mirror mode turbulence in the Earth's magnetosheath

A. Osmane[1], A. P. Dimmock[1], and T. I. Pulkkinen[1]

[1]Department of Radio Science and Engineering, Aalto University, Espoo, Finland

Abstract We use more than 7 years of Time History of Events and Macroscale Interactions during Substorms observations to quantify the non-Gaussian properties associated with mirror mode turbulence in the Earth's magnetosheath. We find that non-Gaussian statistics of mirror modes lead to the parabolic collapse of kurtosis as the square of the skewness ($K = aS^2 + B$ with $a \sim 1.3$ and $b \sim -1$). The parabolic scaling is a global constraint for the magnetosheath and is dictated by kinetic processes. This parabolic scaling is qualitatively independent of the distance to the magnetopause or bow shock, which implies that, even though the bow shock is driving the mirror mode instability, the dynamical evolution of mirror structures is independent of the source region and due to local processes. The parabolic relationship and coefficients between kurtosis and skewness for mirror modes in the Earth's magnetosheath are also similar to those found in a wide range of geophysical and laboratory turbulent environments, providing further evidence that turbulent systems dominated by non-Gaussian fluctuations hold universal statistical properties.

1. Introduction

More than half a century after the first theoretical studies of mirror mode instabilities [*Chandrasekhar et al.*, 1958; *Shapiro and Shevchenko*, 1963; *Hasegawa*, 1969], observational discoveries [*Kaufmann and Horng*, 1971], and subsequent detections within a wide range of space plasmas [*Tsurutani et al.*, 1982; *Neubauer et al.*, 1993; *Sahraoui et al.*, 2004; *Joy et al.*, 2006; *Génot*, 2008; *Génot et al.*, 2009; *Soucek et al.*, 2008], fundamental questions associated with the nonlinear saturation [*Kuznetsov et al.*, 2007; *Southwood and Kivelson*, 1993], and global properties [*Johnson and Cheng*, 1997] of mirror modes in planetary magnetosheaths remain actively investigated. Kinetic by nature, mirror modes are spontaneously generated as a consequence of pressure anisotropies and therefore commonly occur in collisionless and magnetized high $\beta = 2\mu_0 n k_B T/B^2$ plasmas. In planetary magnetosheaths, a dominant source for such temperature anisotropy is provided by the heating at the bow shock [*Kulsrud*, 2005], whereas in weakly collisional galactic plasmas, pressure anisotropies are sustained by turbulent motion [*Schekochihin et al.*, 2008].

Despite their kinetic scales, mirror modes are central to the global- and large-scale structures of planetary magnetosheaths. It has been established that nonlinear mirror modes affect the large-scale properties of the Earth's magnetosheath plasma [*Soucek et al.*, 2008] and dominate the turbulent energy spectra up to 1.4 Hz [*Sahraoui et al.*, 2004]. Theoretical studies also indicate that mirror modes can couple a significant amount of energy from the magnetosheath to the magnetopause and result in additional plasma transport into the magnetosphere [*Johnson and Cheng*, 1997].

Mirror mode structures typically appear as quasi-stationary dips or peaks in the plasma frame, with little or no change in the mean magnetic field direction. Consequently, mirror mode signatures in probability distribution functions (PDF) of magnetic field fluctations are observed in the form of tails [*Génot et al.*, 2009; *Soucek et al.*, 2008] and represent a departure from Gaussian statistics. In this *Letter*, we quantify the statistical departure from Gaussianity caused by mirror mode turbulence by computing the third and fourth moments of the PDF as a function of the distance from the magnetopause. Put differently, we are interested in the global constraints on the Earth's magnetosheath imposed by the dynamical evolution of kinetic mirror modes into coherent structures. The unveiling of global constraints driven by kinetic scales are particularly relevant to recent efforts to develop space weather models, taking into account ion kinetic processes [*Karimabadi et al.*, 2006; *Alfthan et al.*, 2014; *Karimabadi et al.*, 2014]. In the case of the Earth's magnetosheath, it means determining the mechanisms through which mirror mode structures regulate the macroscale properties of the plasma.

The outline of this *Letter* is as follows: in section 2 we describe the methodology of the Time History of Events and Macroscale Interactions during Substorms (THEMIS) data analysis and the detection algorithm of mirror structures. In section 3 we present the statistical relationship of higher-order moments of the PDF for mirror modes and focus specifically on the evolution of non-Gaussian moments as function of distance from the magnetospheric boundaries. We show that non-Gaussian mirror fluctuations result in the parabolic collapse of kurtosis into skewness. In section 4 we discuss the significance of this collapse in relation to similar results in plasma and geophysical turbulent systems. We conclude by noting a number of limitations and directions for future work.

2. Methodology

2.1. Data Sets and Instrumentation

The statistical database of magnetosheath observations is compiled from measurements collected by the array of instrumentation on board the THEMIS spacecraft [*Angelopoulos*, 2008] between October 2007 and December 2013. Magnetic field measurements are obtained by the FluxGate Magnetometer (FGM) on board each probe [*Auster et al.*, 2008] and since mirror modes can be observed at time scales starting from about 4 s [*Soucek et al.*, 2008], we use the 4 Hz resolution data. Ion temperatures, necessary to compute the mirror mode linear instability criterion, are obtained through the electrostatic analyzer instrument [*McFadden et al.*, 2008].

2.2. Magnetosheath Mapping

To compile the database of mirror mode properties we apply a previously developed statistical mapping tool [*Dimmock and Nykyri*, 2013; *Dimmock et al.*, 2014]. The tool transforms to each THEMIS data point initially in the Geocentric Solar Ecliptic frame to the magnetosheath interplanetary medium (MIPM) reference frame [*Verigin et al.*, 2006]. Each data point in the MIPM frame is a function of the upstream interplanetary magnetic field (IMF) vector which effectively rearranges data points with respect to the geometry of the bow shock. As a result, the dawn and dusk flanks always correspond to a bow shock in the quasi-parallel and quasi-perpendicular regimes, respectively. Each MIPM data point is then normalized across the model magnetosheath using the solar wind-dependent bow shock model by *Verigin et al.* [2006] and the magnetopause model by *Shue et al.* [1998]. The fractional distance (F) across the magnetosheath ranges from 0 at the magnetopause to 1 at the bow shock (points greater than 1 or smaller than 0 are discarded). The purpose of this process is to allow direct comparison of measurements made under different conditions at the shock and in the upstream solar wind and IMF. To evaluate each model and MIPM location, we use a 20 min mean average of the OMNI data for an estimate of the upstream conditions. For magnetosheath properties, a 3 min window is selected about each point which is then used to perform the analysis for each relevant parameter. Although we do not focus on dawn/dusk asymmetries in the present study, the MIPM frame provides an efficient method to isolate magnetosheath measurements from the THEMIS data. The benefit of this frame is that when we compute the coefficients of the *K-S* curves as a function of magnetopause distance, the MIPM frame accounts for the asymmetrical thickness of the shock on the dawn and dusk flanks.

2.3. Mirror Mode Selection Criteria

We apply the following criteria to determine whether mirror structures are observed in the magnetosheath plasma sampled during 7 years by THEMIS. Mirror modes are almost linearly polarized and compressive; hence, their maximum variance ($\vec{\mathbf{B}}_m$) direction, unlike for almost transverse waves, should not lie too far from the average magnetic field direction ($\vec{\mathbf{b}}_0$). For these reasons our analysis is performed on the modulus of the magnetic field data and not the individual components. For each 3 min interval, we compute both $\vec{\mathbf{b}}_0 = \left[\bar{B}_x, \bar{B}_y, \bar{B}_z\right]/|\bar{B}_x, \bar{B}_y, \bar{B}_z|$ and using minimum variance analysis [*Sonnerup and Cahill*, 1967], we determine $\vec{\mathbf{B}}_m$. The angle between $\vec{\mathbf{B}}_m$ and $\vec{\mathbf{b}}_0$ is calculated (θ_{bm}), and for mirror modes to occur, the condition $\theta_{bm} < 30°$ is required. To ensure a reliable estimate of $\vec{\mathbf{B}}_m$, the eigenvalues of the maximum (λ_{max}), intermediate (λ_{int}), and minimum (λ_{min}) variance directions are considered. Similar to *Soucek et al.* [2008], we require that $\lambda_{\mathrm{max}}/\lambda_{\mathrm{int}} > 1.5$ and $\lambda_{\mathrm{int}}/\lambda_{\mathrm{min}} > 0.3$ for an interval to be considered. We also require the instability threshold condition derived by *Hasegawa* [1969] for cold electrons, in terms of the ion temperature anisotropy $T_\perp/T_\parallel$ and the perpendicular plasma $\beta_\perp$, to hold. The instability threshold is expressed as follows:

$$C_m = \frac{T_\perp}{T_\parallel} - \frac{1}{\beta_\perp} - 1 > 0. \tag{1}$$

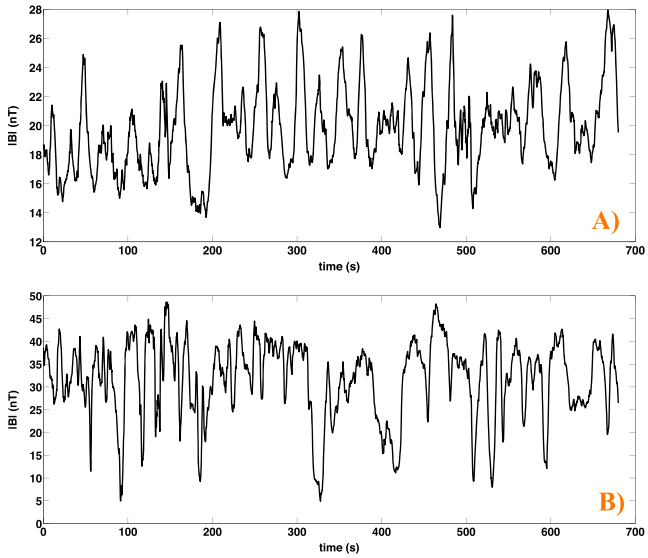

Figure 1. Examples of 11 min time series dominated by (a) peaks and (b) dips. These intervals have been found with our algorithm under the conditions described in section 2.3.

Figure 1 shows two 11 min intervals of FGM data where mirror modes were identified by the above selection criteria. Mirror modes come in two "flavors", appearing either as dips or peaks in the magnetic field amplitude [*Génot et al.*, 2009; *Soucek et al.*, 2008]. Figure 1a corresponds to an interval of FGM data dominated by peaks, whereas Figure 1b represents another interval heavily influenced by dips. Even though our study is substantially different in its motivation than that of *Soucek et al.* [2008] and *Génot et al.* [2009], we have validated our selection criteria by comparing our data sets with theirs. The statistical properties observed from our data set (not shown below) match exactly those by *Soucek et al.* [2008] and *Génot et al.* [2009], even though the studies differ by spacecraft, time period, window length, and FGM resolution. This degree of similarity is suggestive of robust statistical properties of mirror modes.

2.4. Non-Gaussian Statistics

When an interval is deemed as a candidate for the mirror mode instability, we calculate the skewness and kurtosis of the magnetic field data for each 3 min window. Since mirror modes manifest as peaks or dips, they produce tails in the distribution which result in positive skewness for peaks and negative skewness for dips. The skewness is defined as follows:

$$S = \frac{M_3}{\sigma^3}, \tag{2}$$

$$M_3 = \frac{1}{N}\sum_{i=1}^{N}\left(B_i - \bar{B}\right)^3, \tag{3}$$

and variance σ. We complement our study of the non-Gaussian properties of mirror mode turbulence by computing the excess kurtosis from the fourth moment of the distribution function as follows:

$$K = \frac{M_4}{\sigma^4} - 3, \tag{4}$$

$$M_4 = \frac{1}{N}\sum_{i=1}^{N}\left(B_i - \bar{B}\right)^4. \tag{5}$$

The excess kurtosis, or flatness, is indicative of the probability of large fluctuations and can be indicative of intermittency [*Krommes*, 2002]. A probability distribution function with longer tails will therefore have a larger kurtosis than a PDF with narrower tails. We complement our analysis by eliminating from our data sets values of the kurtosis and skewness that were not significantly different than 0, that is, values that are not significantly different from Gaussian fluctuations. The standard errors of skewness and kurtosis are approximately

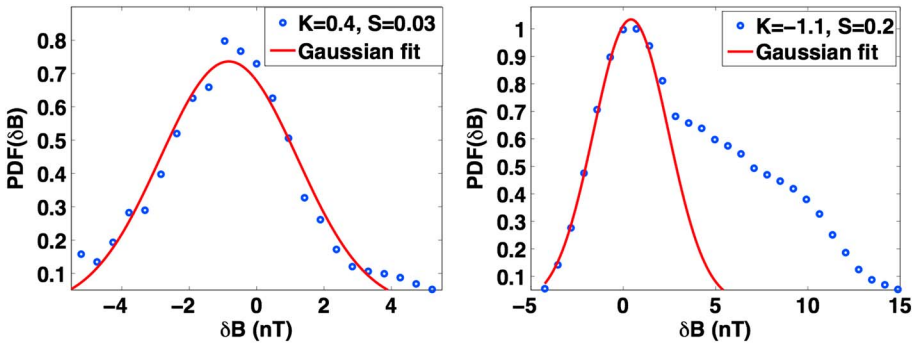

Figure 2. Two examples of PDF of the magnetic field fluctuations δB. (left) One for an interval that did not fit the criteria for mirror mode fluctuations with a kurtosis and skewness not significantly different than 0, i.e., $\sigma_K = \pm 0.4$ and $\sigma_S = \pm 0.2$. (right) PDF that possesses a kurtosis significantly different than 0 and is counted as a mirror event. The kurtosis and the skewness of the mirror mode interval are greater and consequently results in more pronounced non-Gaussian statistics.

$\sigma_{\text{skew}} = \sqrt{6/N}$ and $\sigma_{\text{kurt}} = \sqrt{24/N}$ [*Sura and Sardeshmukh*, 2008], where N is the effective number of independent observations. In our case the kurtosis and skewness is computed from 3 min windows sampled at 4 Hz, resulting in $\sigma_{\text{skew}} \sim 0.1$ and $\sigma_{\text{kurt}} \sim 0.2$. We reject values of K-S that fit inside the box $[\pm 2\sigma_{\text{kurt}}, \pm 2\sigma_{\text{skew}}]$ corresponding to a 95% confidence interval. This procedure reduces our data sets by $\sim$ 2% but does not modify our results and conclusions and has the benefit to only preserve non-Gaussian mirror mode fluctuations. Any departure from zero kurtosis (as defined above) and skewness indicates statistics which are non-Gaussian. Figure 2 shows two examples of PDF of the magnetic field fluctuations δB. Figure 2 (left) is one for an interval that did not fit the statistical criteria for non-Gaussian mirror mode fluctuations, whereas Figure 2 (right) did.

3. Results and Discussion

3.1. *K-S* Relationship of Mirror Modes

Our first result is illustrated in Figure 3 that shows the statistical results of kurtosis versus skewness of the mirror mode fluctuations for the $N = 50{,}623$ three minute intervals identified from the 7 years of THEMIS observations. Each data point is plotted as a blue dot. A least squares fit shows that the relationship between kurtosis and skewness is given by a parabola that can be written as $K = aS^2 + b$. The red curve is the best fit resulting in a parabola $K = 1.32S^2 - 1.03$ with R squared value of 91%. It should be pointed out that the addition of a linear $\sim c \times S$ and/or cubic $d \times S^3$ term to the K-S fit does not improve the R squared value. If linear and/or cubic terms are added, one finds coefficients of the order 0.01. The use of a purely parabolic relationship between kurtosis and skewness, therefore, simplifies our analysis without biasing our results. The errors on the parameters a and b are then computed by taking the maximum dispersion for the 95% confidence interval of the least squares fit.

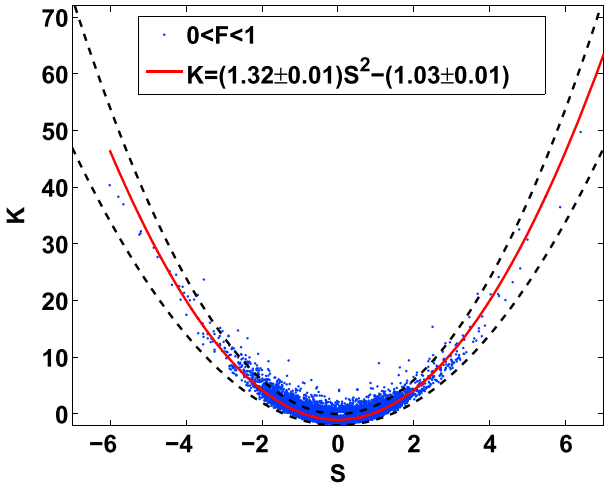

Figure 3. Kurtosis versus skewness of mirror mode fluctuations for 7 years of THEMIS measurements. The blue dots represent the data points. The red line is the best fit resulting in a parabola $K = 1.32S^2 - 1.03$. The black dotted curves represent the constraint on kurtosis versus skewness for Beta distributions. Ninety-six percent of the K-S cloud is comprised between those two curves.

It is interesting to note that the parabolic shape of the K-S curve of mirror mode structures has been observed in physical systems with a priori no relationship with turbulent magnetosheath plasma. The measured coefficient, $a = 1.3$ is of comparable magnitude to those observed in sea surface temperature fluctuations and

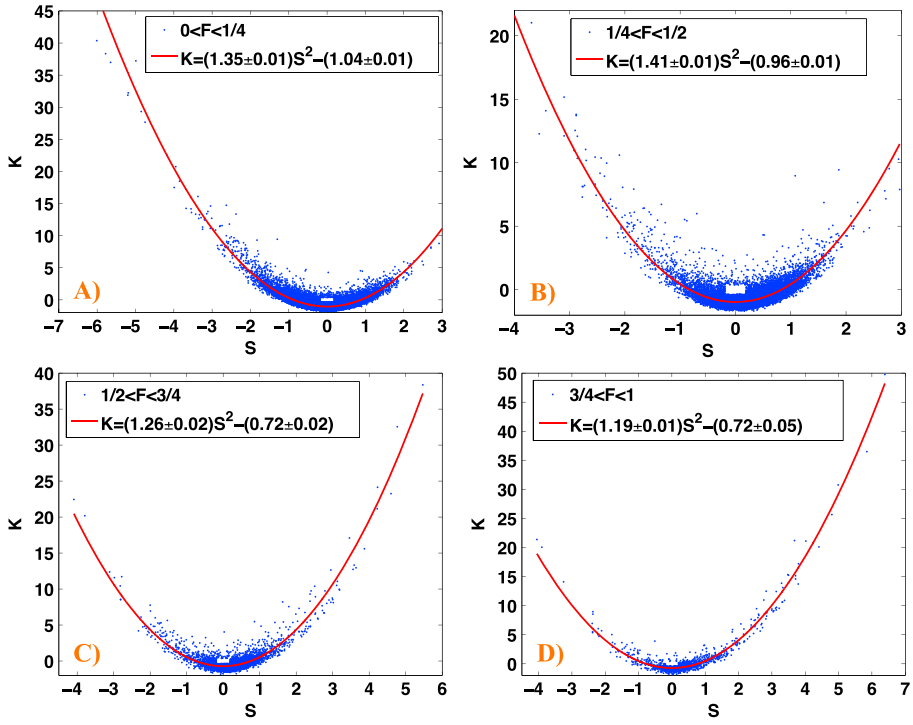

Figure 4. Kurtosis versus skewness of mirror modes plotted for the fractional distance F. (a) For $0 < F < 1/4$, i.e., the closest to the magnetopause. (b) For mirror modes observed between $1/4 < F < 1/2$; (c) events observed between $1/2 < F < 3/4$. (d) For mirror modes observed near the shock, i.e., $1 > F > 3/4$. Note that the scales on each panel vary. The fitted curves, resulting in parabolas, for each panel, are qualitatively similar for various fractional distances. Large peaks (positive skewness) are observed mostly near the shock (Figure 4d), and large dips (negative skewness) are observed mostly near the magnetopause (Figure 4a). The parameters for the parabola (a, b) are also observed to increase as one approaches the magnetopause.

laboratory plasmas [*Sura and Sardeshmukh*, 2008; *Labit et al.*, 2007]. As pointed out by several authors before [*Sura and Sardeshmukh*, 2008; *Labit et al.*, 2007; *Sandberg et al.*, 2009; *Krommes*, 2008; *Hamza and Meziane*, 2011], the similar statistical features of non-Gaussian processes among different physical systems indicate that these systems can be described by the same stochastic differential equations and thus share universal properties.

The black dashed curves in Figure 3 represent the constraint on kurtosis versus skewness for Beta distributions [*Labit et al.*, 2007]. We find that 96% of K-S measurement pairs fall between the constraints on the kurtosis and skewness for Beta distributions:

$$S^2 - 2 \le K \le \frac{3}{2}S^2. \tag{6}$$

While the Beta distributions have been used before to characterize laboratory plasma turbulence [*Labit et al.*, 2007] and the collapse of the K-S curve is appropriately constrained by Beta distributions, there is no physical justification for its use but provides an empirical constraint for theoretical modeling [*Sura and Sardeshmukh*, 2008; *Krommes*, 2008]. We also note that the simpler stochastic model developed by *Sandberg et al.* [2009] to explain the K-S curves of non-Gaussian processes cannot be used for mirror mode turbulence. This is because dips and peaks are mixed during some mirror intervals, which results in symmetric distribution with fat tails and, statistically, nonzero kurtosis for zero skewness $K(S = 0) \neq 0$.

3.2. *K-S* Relationship as a Function of Distance From the Bow Shock and Magnetopause

Mirror modes are spontaneously generated as a consequence of pressure anisotropies. In the context of planetary magnetosheaths, the bow shock is the dominant source for such pressure anisotropies. As the magnetic field is compressed and the perpendicular velocity is converted into gyromotion, a large perpendicular temperature is generated [*Kulsrud*, 2005]. Since the motion along the magnetic field does not experience similar enhancement, a $T_\perp > T_\parallel$ anisotropy develops. It is therefore of interest for the global properties of mirror modes to determine the evolution of the K-S curve as a function of distance to the bow shock.

Figure 4 shows the kurtosis versus the skewness as a function of the fractional distance (F) from the magnetopause. A value of 0 corresponds to the magnetopause boundary, and a value of 1 corresponds to the bow shock. Figure 4a is for $F < 1/4$, i.e., the closest to the magnetopause. Figure 4b is for mirror modes observed between $1/4 < F < 1/2$ and Figure 4c for events observed between $1/2 < F < 3/4$. Figure 4d is for mirror modes observed near the shock, i.e., $1 > F > 3/4$. The least squares fitted curves, resulting in parabolas for each panel, are qualitatively similar for various fractional distances. However, a number of differences in the parabolic collapse of the K-S curve can be noted as a function of F. We note that peaks (positive skewness) with large amplitudes (high kurtosis, i.e., $K > 5$) are mostly observed near the bow shock, whereas dips (negative skewness) with large amplitudes (high kurtosis, i.e., $K > 5$) are mostly observed deep in the magnetosheath near the magnetopause. We also note that the parabolas are wider and the kurtosis at zero skewness $K(S = 0)$ are larger near the magnetopause than closer to the bow shock. In the center of the magnetosheath ($1/3 > F > 2/3$) we observe a mixture of dips and peaks with high kurtosis but with a greater number of dips than peaks. The distribution of peaks and dips as a function of fractional distance is therefore consistent with previous studies [*Génot et al.*, 2009; *Soucek et al.*, 2008, and references therein].

The change in the parabola parameters from the shock toward the magnetopause indicates that, statistically, mirror mode turbulence reaches greater levels of non-Gaussianity away from the source region. The mirror mode turbulence remains highly non-Gaussian, but the effect is further enhanced deep in the magnetosheath. This result provides an additional benchmarking constraint for numerical studies of magnetosheath turbulence and, on the other hand, could be explained by numerical studies of mirror mode saturation mechanisms taking into account boundary effects [*Johnson and Cheng*, 1997].

4. Conclusion

We have used more than 7 years of THEMIS observations to quantify the non-Gaussianity of the plasma distribution associated with mirror mode turbulence in the Earth's magnetosheath. We found that non-Gaussian fluctuations associated with mirror modes have the property that the kurtosis can be given as the square of the skewness. The parabolic collapse of the K-S curve with coefficients ($a \sim 1.3, b \sim -1$) provides a global constraint sustained by local/kinetic processes of magnetosheath models. Our results are particularly relevant for recent global modeling efforts that incorporate ion kinetic effects in large-scale space weather models [*Karimabadi et al.*, 2006; *Alfthan et al.*, 2014; *Karimabadi et al.*, 2014]. Kinetic simulations trying to reproduce kinetic properties of the magnetosheath plasma could use our results as a mean to benchmark the plasma state. Spanning 7 years of magnetosheath measurements, our results are statistically significant and demonstrate a clear relationship between kurtosis and skewness for plasma embedded by mirror mode fluctuations.

The parabolic scaling $K = aS^2 + b$ is qualitatively independent of the proximity to the magnetopause or bow shock boundaries, implying that even though the more variable bow shock is driving mirror mode instabilities, the dynamical evolution of non-Gaussian fluctuations is due to local processes. Quantitatively, the absolute value of kurtosis increases on average as one approaches the magnetopause for zero and nonzero values of the skewness, that is, the increase of the absolute value of the coefficients (a, b) toward the magnetopause indicates that, statistically, the mirror mode turbulence is more non-Gaussian farther away from the bow shock source region.

The relationship between kurtosis and skewness and the associated coefficients for mirror modes in the Earth's magnetosheath is similar to those found in a wide range of turbulent environments with no apparent physical connections [*Labit et al.*, 2007; *Sura and Sardeshmukh*, 2008; *Hamza and Meziane*, 2011; *Mezaoui et al.*, 2014]. Consequently, our results provide additional evidence that, despite inherently different physical processes, geophysical turbulent systems dominated by second-order nonlinearities might hold universal statistical properties and be explained under a combined mathematical formalism.

Finally, we would like to stress a caveat to our study. Mirror modes are not the only coherent structures in the magnetosheath leading to possible departures from Gaussian statistics [*Alexandrova*, 2008; *Hietala et al.*, 2009; *Archer and Horbury*, 2013]. Computing the kurtosis and skewness for events that do not fit our mirror mode criteria also results in a parabolic scaling, albeit one with significantly different coefficients ($a \to 3/2, b \to 0$) and with a linear term $\sim 0.1S$ denoting antisymmetry between positive and negative skewness of non-Gaussian structures. Our analysis, however, is solely focused on linearly unstable mirror turbulence because of its central role in regulating the collisionless magnetosheath plasma. A study of magnetosheath turbulence taking

into account other coherent structures such as pressure pulses and Alfvén vortices could form the basis of future studies. Additionally, future theoretical and numerical work investigating the saturation and evolution of mirror modes in the magnetosheath, as well as the impact of the boundaries, will be required to include an analysis for the rise and collapse of the *K*-*S* curve in the form observed by the 7 year THEMIS mission.

Acknowledgments
This work was supported by the Academy of Finland grant 267073/2013. The OMNI data were obtained for free from the GSFC/SPDF OMNIWeb interface at http://omniweb.gsfc.nasa.gov. We acknowledge NASA contract NAS5-02099 and V. Angelopoulos for use of data from the THEMIS Mission. THEMIS data are available for free at http://themis.igpp.ucla.edu/overview_data.shtml.

The Editor thanks two anonymous reviewers for their assistance in evaluating this paper.

References

Alexandrova, O. (2008), Solar wind vs magnetosheath turbulence and Alfvén vortices, *Nonlinear Processes Geophys.*, *15*(1), 95–108.
Alfthan, S., D. Pokhotelov, Y. Kempf, S. Hoilijoki, I. Honkonen, A. Sandroos, and M. Palmroth (2014), Vlasiator: First global hybrid-Vlasov simulations of Earth's foreshock and magnetosheath, *J. Atmos. Sol. Terr. Phys.*, *120*, 24–35, doi:10.1016/j.jastp.2014.08.012.
Angelopoulos, V. (2008), The THEMIS mission, *Space Sci. Rev.*, *141*, 5–34, doi:10.1007/s11214-008-9336-1.
Archer, M., and T. Horbury (2013), Magnetosheath dynamic pressure enhancements: Occurrence and typical properties, *Ann. Geophys.*, *31*(2), 319–331.
Auster, H. U., et al. (2008), The THEMIS fluxgate magnetometer, *Space Sci. Rev.*, *141*, 235–264, doi:10.1007/s11214-008-9365-9.
Chandrasekhar, S., A. N. Kaufman, and K. M. Watson (1958), The stability of the pinch, *Proc. R. Soc. A*, *245*, 435–455, doi:10.1098/rspa.1958.0094.
Dimmock, A. P., and K. Nykyri (2013), The statistical mapping of magnetosheath plasma properties based on THEMIS measurements in the magnetosheath interplanetary medium reference frame, *J. Geophys. Res. Space Physics*, *118*, 4963–4976, doi:10.1002/jgra.50465.
Dimmock, A. P., K. Nykyri, and T. I. Pulkkinen (2014), A statistical study of magnetic field fluctuations in the dayside magnetosheath and their dependence on upstream solar wind conditions, *J. Geophys. Res. Space Physics*, *119*, 6231–6248, doi:10.1002/2014JA020009.
Génot, V. (2008), Mirror and firehose instabilities in the heliosheath, *Astrophys. J. Lett.*, *687*(2), L119, doi:10.1086/593325.
Génot, V., E. Budnik, C. Jacquey, I. Dandouras, and E. Lucek (2009), Mirror modes observed with Cluster in the Earth's magnetosheath: Statistical study and IMF/solar wind dependence, *Adv. Geosci.*, *14*, 263–283.
Hamza, A. M., and K. Meziane (2011), On turbulence in the quasi-perpendicular bow shock, *Planet. Space Sci.*, *59*, 475–481, doi:10.1016/j.pss.2010.03.013.
Hasegawa, A. (1969), Drift mirror instability of the magnetosphere, *Phys. Fluids*, *12*, 2642–2650, doi:10.1063/1.1692407.
Hietala, H., T. V. Laitinen, K. Andréová, R. Vainio, A. Vaivads, M. Palmroth, T. I. Pulkkinen, H. E. J. Koskinen, E. A. Lucek, and H. Rème (2009), Supermagnetosonic jets behind a collisionless quasiparallel shock, *Phys. Rev. Lett.*, *103*(24), 245,001, doi:10.1103/PhysRevLett.103.245001.
Johnson, J. R., and C. Cheng (1997), Global structure of mirror modes in the magnetosheath, *J. Geophys. Res.*, *102*(A4), 7179–7189.
Joy, S. P., M. G. Kivelson, R. J. Walker, K. K. Khurana, C. T. Russell, and W. R. Paterson (2006), Mirror mode structures in the Jovian magnetosheath, *J. Geophys. Res.*, *111*, A12212, doi:10.1029/2006JA011985.
Karimabadi, H., H. Vu, D. Krauss-Varban, and Y. Omelchenko (2006), Global hybrid simulations of the Earth's magnetosphere, in *Numerical Modeling of Space Plasma Flows*, vol. 359, edited by N. V. Pogorelov and and G. P. Zank, p. 257, Astron. Soc. of the Pacific, San Francisco, Calif.
Karimabadi, H., et al. (2014), The link between shocks, turbulence, and magnetic reconnection in collisionless plasmas, *Phys. Plasmas*, *21*(6), 62,308, doi:10.1063/1.4882875.
Kaufmann, R. L., and J.-T. Horng (1971), Physical structure of hydromagnetic disturbances in the inner magnetosheath, *J. Geophys. Res.*, *76*, 8189, doi:10.1029/JA076i034p08189.
Krommes, J. A. (2002), Fundamental statistical descriptions of plasma turbulence in magnetic fields, *Phys. Reps.*, *360*(1), 1–352.
Krommes, J. A. (2008), The remarkable similarity between the scaling of kurtosis with squared skewness for TORPEX density fluctuations and sea-surface temperature fluctuations, *Phys. Plasmas*, *15*(3), 30,703.
Kulsrud, R. (2005), *Plasma Physics for Astrophysics*, Princeton Univ. Press, N. J.
Kuznetsov, E. A., T. Passot, and P. L. Sulem (2007), Dynamical model for nonlinear mirror modes near threshold, *Phys. Rev. Lett.*, *98*, 235,003, doi:10.1103/PhysRevLett.98.235003.
Labit, B., I. Furno, A. Fasoli, A. Diallo, S. H. Müller, G. Plyushchev, M. Podestà, and F. M. Poli (2007), Universal statistical properties of drift-interchange turbulence in TORPEX plasmas, *Phys. Rev. Lett.*, *98*, 255,002, doi:10.1103/PhysRevLett.98.255002.
McFadden, J. P., C. W. Carlson, D. Larson, M. Ludlam, R. Abiad, B. Elliott, P. Turin, M. Marckwordt, and V. Angelopoulos (2008), The THEMIS ESA plasma instrument and in-flight calibration, *Space Sci. Rev.*, *141*, 277–302, doi:10.1007/s11214-008-9440-2.
Mezaoui, H., A. Hamza, and P. Jayachandran (2014), Investigating high-latitude ionospheric turbulence using global positioning system data, *Geophys. Res. Lett.*, *41*, 6570–6576, doi:10.1002/2014GL061331.
Neubauer, F., K.-H. Glassmeier, A. Coates, and A. Johnstone (1993), Low-frequency electromagnetic plasma waves at comet P/Grigg-Skjellerup: Analysis and interpretation, *J. Geophys. Res.*, *98*, 937–953.
Sahraoui, F., G. Belmont, J. Pinçon, L. Rezeau, A. Balogh, P. Robert, and N. Cornilleau-Wehrlin (2004), Magnetic turbulent spectra in the magnetosheath: New insights, *Ann. Geophys.*, *22*, 2283–2288, doi:10.5194/angeo-22-2283-2004.
Sandberg, I., S. Benkadda, X. Garbet, G. Ropokis, K. Hizanidis, and D. Del-Castillo-Negrete (2009), Universal probability distribution function for bursty transport in plasma turbulence, *Phys. Rev. Lett.*, *103*(16), 165,001, doi:10.1103/PhysRevLett.103.165001.
Schekochihin, A., S. Cowley, R. Kulsrud, M. Rosin, and T. Heinemann (2008), Nonlinear growth of firehose and mirror fluctuations in astrophysical plasmas, *Phys. Rev. Lett.*, *100*(8), 81,301.
Shapiro, V., and V. Shevchenko (1963), Quasilinear theory of instability of a plasma with an anisotropic ion velocity distribution, *Zh. Eksperim. i Teor. Fiz.*, *45*, 1612.
Shue, J.-H., et al. (1998), Magnetopause location under extreme solar wind conditions, *J. Geophys. Res.*, *103*, 17,691–17,700, doi:10.1029/98JA01103.
Sonnerup, B. U. O., and L. J. Cahill Jr. (1967), Magnetopause structure and attitude from Explorer 12 observations, *J. Geophys. Res.*, *72*, 171–183, doi:10.1029/JZ072i001p00171.
Soucek, J., E. Lucek, and I. Dandouras (2008), Properties of magnetosheath mirror modes observed by Cluster and their response to changes in plasma parameters, *J. Geophys. Res.*, *113*, A04203, doi:10.1029/2007JA012649.
Southwood, D. J., and M. G. Kivelson (1993), Mirror instability: I. Physical mechanism of linear instability, *J. Geophys. Res.*, *98*, 9181–9187, doi:10.1029/92JA02837.
Sura, P., and P. D. Sardeshmukh (2008), A global view of non-Gaussian SST variability, *J. Phys. Oceanogr.*, *38*, 639–647, doi:10.1175/2007JPO3761.1.

Tsurutani, B. T., E. J. Smith, R. R. Anderson, K. W. Ogilvie, J. D. Scudder, D. N. Baker, and S. J. Bame (1982), Lion roars and nonoscillatory drift mirror waves in the magnetosheath, *J. Geophys. Res.*, *87*, 6060–6072, doi:10.1029/JA087iA08p06060.

Verigin, M. I., M. Tátrallyay, G. Erdos, and G. A. Kotova (2006), Magnetosheath interplanetary medium reference frame: Application for a statistical study of mirror type waves in the terrestrial plasma environment, *Adv. Space Res.*, *37*, 515–521, doi:10.1016/j.asr.2005.03.042.